CHAPTER III

THEORY

Alumina is an important material in many fields because of its excellent and wide range properties. Study of alumina has been a subject of great interest for many decades. It is one of the most common crystalline materials to be used as adsorbent, coating, soft abrasives, catalyst and catalyst support [92-93] because of its fine particle size, high surface area, and surface catalytic activity.

3.1 Alumina (Al_2O_3)

Alumina is widely used as catalyst, catalyst support, wear-resistance material, ceramic, abrasives, medicinal material, and adsorbent [29, 94], because of its distinctive chemical, mechanical and thermal properties. The details described in this part are based on a review of Levin and Brandon [95] and a text book from Lippens and Steggerda [96].

Alumina is an important material in field of catalytic technology because of its good and important properties. It has high surface area with fine particle size, good adsorbent, catalytic activity, and high melting point (above 2000 °C) which is also desirable for the support. For catalytic applications, alumina can be used in three functions: as catalyst, co-catalyst and support. For example, alumina is used as catalyst in the reaction of steam reforming process at high temperature. Alumina is used as co-catalyst in the catalytic reforming of gasoline and as support in many cases, such as in catalytic converter, in membrane technology etc.

Aluminum trihydroxide ($Al(OH)_3$) and aluminum monohydroxide (AlOOH) exhibit polymorphism and exist in many forms of structure. The structure of all aluminum hydroxides consists of double oxygen layers stacking with the aluminum cations located in octahedrally coordinated interstices. The packing of oxygen ions inside the layer can be either hexagonal or cubic, whereas the symmetry of the overall structure for each hydroxide is determined by the distribution of hydrogen. The relative distance between

hydroxyl groups, both within and between the layers, has been suggested to control the mechanism of dehydration for the particular hydroxide.

3.1.1 Formation and crystal structure of active alumina

Alumina can exist in many metastable phases before transforming to the stable α-alumina (corundum form). There are six principal metastable phases of alumina designated by the Greek letters: chi (χ), kappa (κ), eta (η), theta (θ), delta (δ), and gamma (γ). Although the range of temperature in which each transition phase is thermodynamically stable has been reported by many researchers, they are inconsistent, depending upon various factors such as degree of crystallinity of sample, amount of impurities in the starting materials, and the subsequent thermal history of sample. Most of the studies on phase transformation of alumina was conducted by calcination of alumina precursor. It was found that difference in the phase transformation sequence is resulted from the difference in the precursor structure [97, 98]. Moreover, the transformation sequence is irreversible. The nature of the product obtained by calcination depends on the starting hydroxide and on the calcination condition. The phase transformation sequences, from metastable Al_2O_3 structures to the final stable α-alumina phase, reported in the literature are also approximates.

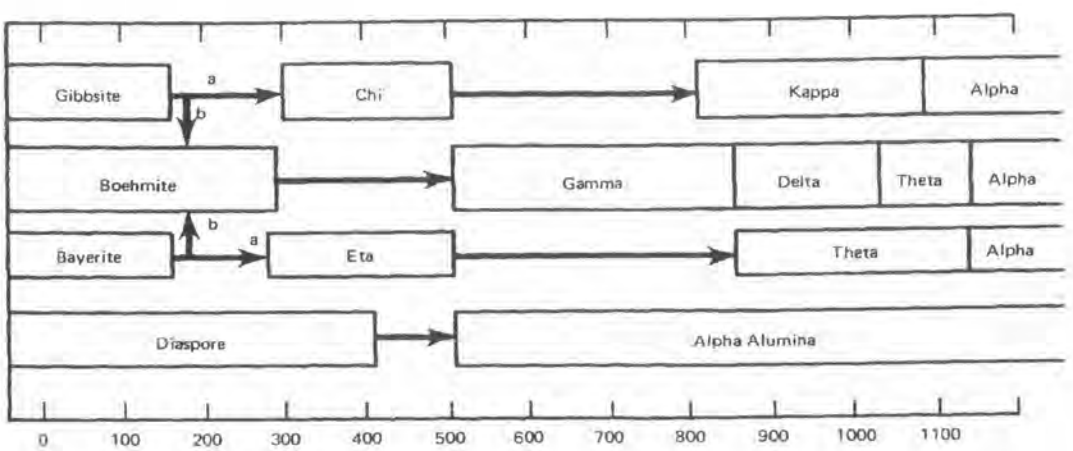

Figure 3.1 Transformation sequence of aluminum hydroxides [30].

The phase transformation sequence normally starts with aluminum hydroxide ($Al(OH)_3$ and AlOOH) transforming to low-temperature phase of alumina (η and χ) at temperature around 150-500°C, and subsequently to high temperature phase (δ, θ, κ) at

temperature around 650-1000°C. Finally, the thermodynamically stable phase, α-alumina, is formed at temperature around 1100-1200°C. It is generally believed that α-phase transformation takes place through the nucleation and growth mechanism.

Aluminas are usually obtained by dehydration of various hydroxides. Much controversy exits about the dehydration of various sequences, even in recent work [29, 94]. Apart from difficulties in characterization of the obtained forms, most of the confusion arises from insufficient information concerning the reaction conditions.

(1) Dehydration of the trihydroxide

The dehydration of gibbsite in air and nitrogen gives the sequence of products different from dehydration of bayerite or nordstrandite. Both crystallinity and particle size of gibbsite are much greater than those of bayerite and nordstrandite. Up to 25% of boehmite can be contaminated by the intergranular hydrothermal reactions in the product from the dehydration of gibbsite, whereas less than 5% is usually formed from bayerite and nordstrandite. However, very fine powders of bayerite [97] and gibbsite do not form any boehmite at all. Detailed phase transformations starting from the trihydroxides are shown in Figure 3.2.

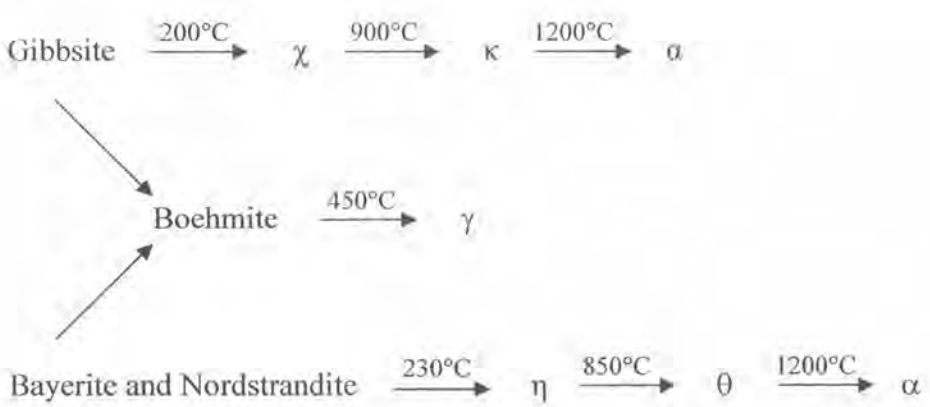

Figure 3.2 Metastable aluminas formed by dehydration of the trihydroxides.

In vacuum, three kinds of trihydroxide decompose at low temperatures into almost completely amorphous product (ρ-alumina), which changes into γ- and η- alumina and further into θ-alumina upon the calcination at high temperature, as shown in Figure 3.3.

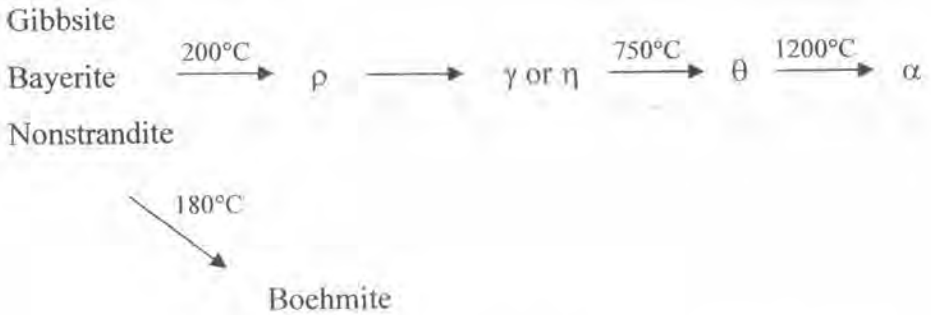

Figure 3.3 Phase transformation of metastable aluminas formed from trihydroxides in vacuum.

(2) Dehydration of oxide hydroxide

Diaspore is the only aluminum hydroxide that transforms directly into α-alumina [99], which initially has high surface area before recrystallization.

The dehydration sequence of boehmite depends on its crystallinity. Well crystallized boehmite (crystal sizes > 1 μ) decomposes according to:

Well crystallized boehmite $\xrightarrow{450°C}$ γ $\xrightarrow{700°C}$ δ $\xrightarrow{1050°C}$ θ+α $\xrightarrow{1200°C}$ α-Al_2O_3

Formation of δ-phase strongly depends on impurities and crystallinity of boehmite. Small amount of Na favors the formation of θ-alumina, whereas Li and Mg stabilize δ-alumina and can prevent the formation of θ-alumina. If boehmite has low crystallinity, the formation of δ-alumina is retarded.

Gelatinous boehmite (pseudoboehmite) decomposes at temperature around 300°C into alumina. Due to the poor crystallinity of the pseudoboehmite, formation of δ-alumina is hardly observed. Thus the dehydration scheme is:

1200 °C

$$\text{Gelatinous boehmite} \xrightarrow{300^{\circ}C} \gamma \xrightarrow{900^{\circ}C} \delta \xrightarrow{1000^{\circ}C} \theta+\alpha \longrightarrow \alpha\text{-}Al_2O_3$$

Gamma alumina is an enormously important material in catalysis. It is used as a catalyst in hydrocarbon conversion (petroleum refining), and as a support for automative and industrail catalysts. It is one of the metastable polymorphs of transition alumina, which is normally obtained by decomposition of boehmite. Boehmite transforms to γ-alumina at temperature in the range of 500-800°C and consequently to δ-alumina at 900°C.

3.2 Selective catalytic reduction of NO_x by hydrocarbon under lean-burn condition

The SCR of nitrogen oxides by hydrocarbons has attracted much attention recently because it has the potential ability to remove nitrogen oxides from diesel exhaust and oxygen rich flue gases. Held et al. [100] and Iwamoto [101] first reported some success using zeolite-based catalyst for lean de-NO_x. However, the hydrothermal resistance of these materials is usually unsatisfactory. After that, the other active catalysts such as platinum group materials (PGMs) [102], based oxide/metals have been investigated as de-NO_x catalyst to improve the stability problem. PGMs are inefficient at moderate and high temperatures, the pioneering work by Hamada et al. [103] and Obuchi et al. [102] described that these metals could catalyze NO_x reduction by hydrocarbon at low temperature (typically below 300°C). Although these catalysts exhibited significant activities for the same reaction, but the problem of selectivity was observed. At low temperature, a significant amount of NO is converted to N_2O rather than N_2. The others base oxides/metals (e.g. Al_2O_3, TiO_2, ZrO_2, MgO and these oxides promoted by, e.g. Co, Ni, Cu, Fe, Sn, Ga, In as well as Ag compounds) are active catalysts for HC-SCR of NO_x [104-108].

Even though some interesting activities were claimed, there is not sufficient evidence for possible application of such systems under real exhaust condition. In fact, even though some increase of thermal/hydrothermal stability could be achieved, the activities are generally poorer compared to the Cu-ZSM5 system. Therefore, many works are focus to find the new catalyst or improve the properties of primary catalysts. Within

several materials, Ag-based catalysts appear to be the most promising materials because they show high activity and selectivity to produce N_2 [68].

Originally, the various promoters including Ag were studied to increase the stability and activity of primary catalysts (zeolite based catalyst). From the literature, clearly the temperatures of highest activity are greatly different dependent on the cations while the maximum activities differed slightly. The order of active temperature regions was Cu < Co < H < Ag < Zn. It was also noted that the wide temperature window over Ag was observed. Moreover, the other metals such as Pd-, Cu- and Au- catalysts are also compared with Ag-based catalyst [105]. In addition, some literature reported regarding unsuccessful improvement of SCR by single phase catalyst [107]. A variety of catalysts including, which can be classified into: zeolites exchanged with metals ions or just a proton types, alumina and its combination with supported metals or metal oxides, metal oxides other than alumina, metal silicates, and ion exchanged materials other than zeolites. Except for emphasizing differences in the activity among catalysts, general behaviors of the catalysts, such as the active temperature range and the selectivity to N_2O, were similar to that investigates under model gas mixture condition. These results led us to the conclusion that the use of any single phase catalyst, including uniformly mixed catalysts composed of two different types of catalyst, does not satisfy the practical demand.

While the improvement of activity is executed, the other study about the stability is made [108-111]. Many works attempted to test the stability because of the typical exhausts to be treated by lean-NO_x catalysts contain up to 10 vol. % of water and up a few hundred parts per million of SO_2. The effect of water on HC-SCR over Ag and other metal promoted on alumina catalyst was investigated. Alumina-supported silver catalyst exhibited extremely high activities in reducing nitric oxide by organic compound in the presence of water [110]. Normally, high concentrations of water in the feed induce a significant deactivation of most catalysts when using light alkenes or alkanes as reductants; however, a high activity can be maintained when oxygenated molecules are used. The inhibition by water is most likely to be due to competitive adsorption between water and one or more of the reactants. The high polarity of oxygenates probably explains their greater ability to compete with water for adsorption when compared to hydrocarbons. Nonetheless, silver has been chosen to study the effect of cocation in order

to limit the migration and the subsequent agglomeration of zeolite based catalyst [109]. The presence of silver is possible to partly prevent the catalyst deactivation and in particular to decrease the inhibiting water effect.

In case of sulphur-tolerance, SO_2 is typically found in lean exhaust streams as a result tolerance of several catalysts. Many published research works reported regarding the SCR of NO_x in the presence of SO_x. An inhibition of the SCR of NO by sulphur dioxide is observed in essentially cases, but its extent dramatically depends on the nature of the reductants and the sulphur concentration. SO_2 is known to react with O_2 and the catalyst surface to form stable sulphate phases under reaction conditions. The formation of these sulphate species brings about a reduction in the number of 'strong' chemisorption sites for NO_x. For Ag-based catalyst, the literature reported both advantage and disadvantage of SO_2. Mostly, the loss of activity for SCR over these catalysts was observed as shown in Figure 3.4 when the SO_2 was introduced into a system. From the DRIFT studies, the spectra of deactivated silver-alumina material showed the formation of two different types of surface sulphate species. One of surface species was a surface aluminum sulphate whereas the other corresponded to a sulphate associated with the silver phases [111]. However, the sulphate species was removed by using the thermal decomposition process. On the other hand, some work [51] found that the N_2 yield in the absence of SO_2 is reached almost instantaneously a constant level, which is considerly lower than in the presence of SO_2. A promotion effect on the catalytic activity was shown in Figure 3.4.

The effect of the other parameter such as space velocity is shown in Figure 3.5. The space velocity affect both NO and C_3H_6 conversion. When the space velocity increase, both NO and C_3H_6 conversion readily decrease. It indicates that the retention time has great effect to the SCR of NO.

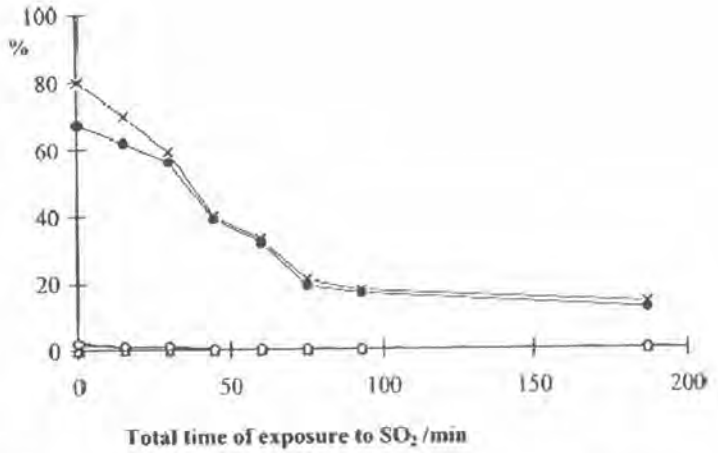

Figure 3.4 N_2 yield (●), N_2O yield (○), NO_2 yield (△) and propene conversion (×) during the propene-SCR of NO over Ag /Al_2O_3 as a function of the time of exposure to 100 ppm of SO_2. T = 486°C, GHSV= 10^5 h^{-1}, 0.1% NO + 0.1% C_3H_6 + 5% O_2 in helium, total flow = 100 ml min^{-1}, 50 mg of catalyst [111].

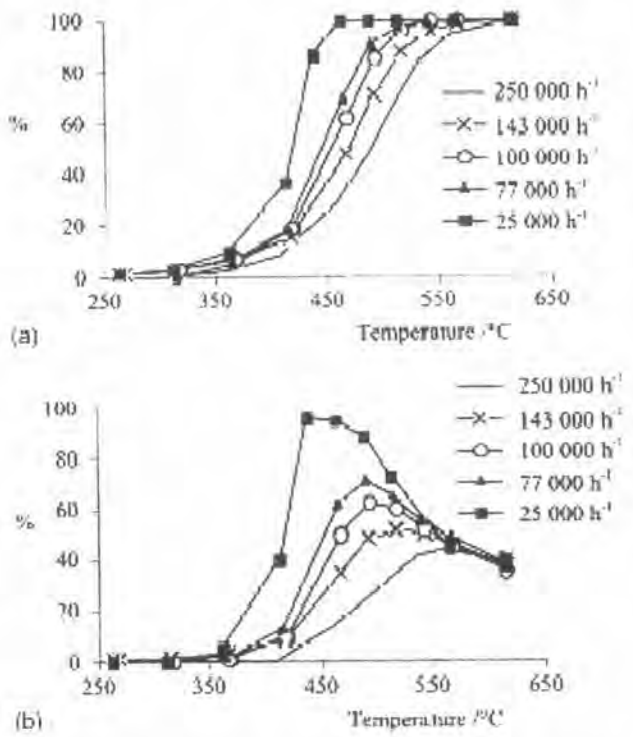

Figure 3.5 (a) Propene conversion and (b) NO conversion to N_2 during the C_3H_6-SCR of NO over 1.2% Ag/Al_2O_3 as a function of temperature and at various GHSV ranging from 25,000 h^{-1} to 250,000 h^{-1}[112].

3.2.1 Reaction Mechanistic Studied

There have been a number studies in which the mechanistic aspects of the selective catalytic reduction of NO by hydrocarbon under excess oxygen on an Ag-based catalyst have been considered but yet there is little definitive evidence in support of one model rather than another and as a consequence several mechanisms have been proposed. In general, the reaction mechanism can be subdivided into decomposition mechanism and reduction mechanism. However, the overall reaction mechanism and the rate-determining step of the selective reduction of NO over a given catalyst depend on the nature of the reductant and the experimental conditions. The mechanism is rather complicated and has not been fully elucidated for any given SCR system. Nevertheless, a general picture of the most significant steps likely to occur during the reaction can be drawn from the vast amount of data generated. Alumina and alumina-supported samples have been the focus of most of the studies of reaction mechanisms, generally using propene as reductant.

The role of dioxygen is quite intricate, as it strongly favours the reduction process over most catalytic formulations [113-114]. Most authors acknowledge that the two main functions of O_2 are the oxidation of NO and of the reductant to form various reaction intermediates. Oxygen may also have a role to play in preventing coking of the catalyst surface, especially in the case of strongly adsorbing hydrocarbons such as alkenes.

Since the reaction orders for N_2 formation with respect to both NO and propene are usually close to zero on alumina-based materials [115], the formation of strongly bound reaction intermediates is expected.

In the absence of O_2, NO only weakly adsorbs on most catalyst surfaces [116-117]. On the contrary, strongly bound nitrite and nitrates are formed in NO/O_2 mixtures. Several literatures reported regarding the reduction of surface species with nitric oxide. Sadykov et al. [118] showed that the decomposition temperatures of strongly bound ad-NO_x species corresponded well to the onset of propane-SCR activity over numerous catalytic formulations. For alumina and silver/alumina, Shimizu et al. [67,119-120] clearly showed that nitrate species were converted to N_2 during exposure to the reductant at rates that were similar to those of the steady-state reduction of NO. These data strongly support the conclusions reached by many research teams on the role of nitrate

species as true reaction intermediates in the SCR process over oxides. The formation of ad-NO_x species on surface sites S is therefore proposed to be the first reaction step of NO as shown in equation 3.1.

$$NO(g) + O_2(g) + S \leftrightarrow \text{ad-}NO_x \tag{3.1}$$

The formation of NO_2 and its role as a reaction intermediate during the SCR reaction has generated much interest. Although the conversion of NO to NO_2 could conceivably be the first step of the CH_4-SCR on some zeolitic materials (e.g. Co/H-ZSM-5 [121]), most selective oxides are not sufficiently active for this reaction to support the formation of NO_2 as a main reaction intermediate.

$$NO(g) + O_2(g) \leftrightarrow NO_2(g) \tag{3.2}$$

Meunier et al. [68] clearly showed that selective SCR catalysts, e.g. low loading (< 2 wt.%) Co or Ag supported on alumina, are not significantly active for either the oxidation of NO to NO_2 or the reverse reaction at the temperatures at which these materials are active for the SCR reaction. The reverse is true for high loading catalysts (e.g. 10 wt.%), which show good activity for NO oxidation, but are nonselective for the SCR reaction. The high rate of NO_2 formation observed over high loading samples is clearly related to their high activity for hydrocarbon combustion. Furthermore, the ratio of NO_2/NO observed during the course of the SCR reaction over selective catalysts sometimes exceeds that associated with the thermodynamic equilibrium value of equation 3.2, clearly discarding it as the main route to NO_2 [66, 68, 122]. High yields of NO_2 can be obtained by the oxidation of organo-nitrito compounds and this rather than the direct oxidation of NO to NO_2 is proposed as the most likely route to gas-phase NO_2 [66, 68].

Similarly to the case of NO, most authors have proposed the formation of strongly bound oxidized species as the first reaction step in the reaction of the hydrocarbon. In addition to the low reaction order for N_2 formation with respect to hydrocarbons [115], this proposition is supported by the fact that oxygenated molecules react much faster and efficiently than hydrocarbons. For the C_3H_6-SCR of NO over alumina and silver/alumina, Shimizu et al. [67, 99, 120] clearly showed that acetate surface species were formed by

the oxidation of various hydrocarbons and were thereafter consumed at rates similar to that of the reduction of NO. The acetate species or other adsorbed oxidised hydrocarbon species are then believed to react with the surface nitrates (and possibly with gas-phase NO_x) to yield organo-nitrogen species, the exact nature of the organo-nitrogen species remains unclear [123-126]. The formation of the organo-nitrogen species is likely to be the rate-determining step of the reaction. These species are not readily detectable but can be observed during carefully designed transient experiments such as temperature-programmed surface reaction monitored by in situ IR. Organo-nitrogen species can be readily formed non-catalytically by reaction of hydrocarbon, dioxygen and nitric oxide in the liquid or gas phase [124]. In addition, the decomposition products of organo-nitrogen species yield similar products to those observed during the SCR reactions (e.g. cyanide, isocyanates), supporting their role as intermediates. The reactivity of nitromethane has been studied over alumina, over which it is readily decomposed below 200 °C forming isocyanate and ammonia species. NH_3 can be obtained from nitromethane through the tautomerisation to the corresponding oxime followed by dehydration to a nitrile N-oxide (equation 3.3), which isomerise to an isocyanate before yielding a primary amine and NH_3 by hydrolysis (equation 3.4), as suggested over zeolitic materials [126]. Over alumina, the possibility of forming NH_3 from reaction of organo-nitrile N-oxides species was confirmed by Obuchi et al. [127]. The same authors proposed that the organo-nitrile N-oxide were formed from organo-nitroso compounds, via enol and cyanide formation (equation 3.5).

$$-CH_2-NO_2 \rightarrow -CH=NO(OH) \rightarrow -C=N=O \qquad (3.3)$$

$$-C=N=O \rightarrow -N=C=O \rightarrow -NH_2 \rightarrow NH_3 \qquad (3.4)$$

$$-CH_2-NO \rightarrow -CH=N(OH) \rightarrow -C\equiv N \rightarrow -C=N=O \qquad (3.5)$$

The selective reduction of NO with ammonia is an efficient reaction over many catalysts, including alumina and other base oxides and metals. The intermediacy of NH_3 in the hydrocarbon-SCR reaction has been suggested over zeolites and alumina-based materials [66]. In addition, isocyanate species, readily formed when hydrocarbon

reductants were used, were also shown to yield N_2 in the presence of O_2 or NO + O_2 [63-66, 128].

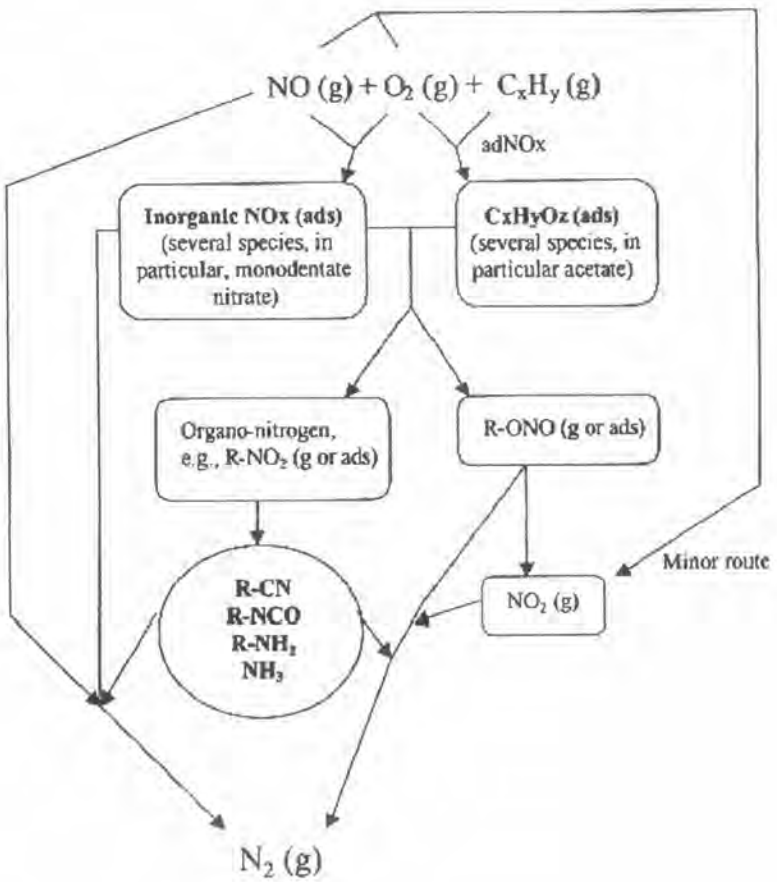

Figure 3.6 Simplified reaction scheme of the C_3H_6-SCR of NO over oxide catalysts giving the nature of the different species likely to be involved. It is proposed that the reduction to N_2 occurs through the reaction of oxidised and reduced (species in shaded circle) nitrogen compounds [66].

It should be noted that the relevance and rate of each step of the scheme represented in Figure 3.6 depends on the nature of the reductant, the catalyst and experimental conditions. The overall rate-determining step and the surface concentrations of each species may vary accordingly. For instance, Shimizu et al. [120] showed that the chain length of the alkane influences their adsorption reaction properties and therefore the rate at which acetates form. As a result, the proportion of the surface coverage of acetates and nitrate species, which compete for surface sites, varies.

3.3 Oxidation of Carbon monoxide

A consistent part of the automotive processes involve the CO oxidation on supported metal catalysts [129]. The materials used in the practical applications are the so-called three-way composite catalysts such as $Pt/Rh/CeO_2/Al_2O_3$, capable of oxidizing CO and hydrocarbons (HC) and reducing nitrogen oxides (NO_x) at the same time [130]. The kinetics of this reaction has been extensively studied. Isothermal temporal oscillations in the CO-oxidation rate were discovered by P. Hugo [131] and M. Jakubith [132] in 1970 on a platinum contact. Similar phenomena on Pt single-crystal surfaces were found by G. Ertl and coworkers on Pt(100) in 1982 [133] and M. Eiswirth and G. Ertl on Pt(110) in 1986 [134]. M.P. Cox and co-workers found a correlation between temporal oscillations and surface structure [135] and by using a scanning-LEED technique were able to observe spatio-temporal patterns [136]. Models of the reaction were implemented to describe temporal [137] and spatio-temporal [138] self-organization patterns arising due to the nonlinear character of this open, far-from-equilibrium system. With the development of dedicated imaging methods (PEEM [139] and EMSI [140]), it became possible to investigate the structures arising from the lateral variations of the concentration of the species at the surface [141].

In the following, the main features of the CO oxidation on platinum (110) are summarized, starting with the description of the single crystal platinum surface, and the characteristics of oxygen and carbon monoxide adsorption on Pt(110) [142]. The coadsorption of both species and the mechanism of the reaction are presented, together with nonlinear effects such as reaction rate oscillations and concentration pattern formation.

3.3.1 The platinum (110) surface

At room temperature the clean (110) surface of a fcc platinum crystal (a = 3.92 Å) (Figure 3.7) displays a different structure than the corresponding bulk planes. The LEED pattern shows a (1×2) reconstruction [143], commonly explained in terms of the missing row model [144] (Figure 3.8): every second (110) close-packed row is absent. The driving force for this rearrangement is the lowering of the surface energy upon the formation of (111) nanofacets.

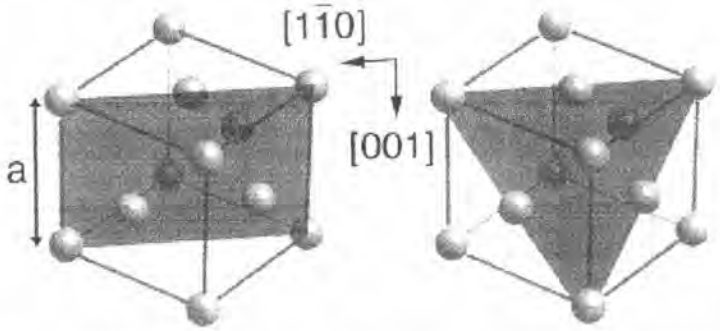

Figure 3.7 The (110) and (111) surfaces of a fcc crystal.[144]

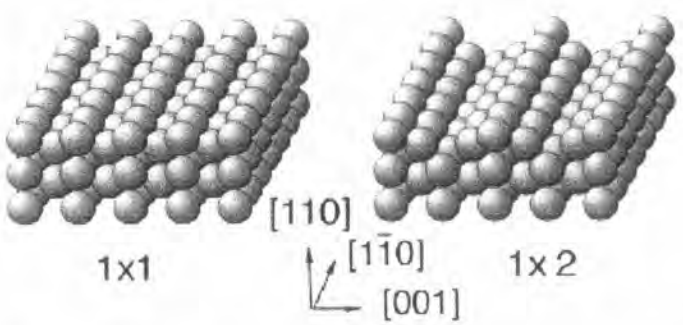

Figure 3.8 The Pt(110) (1×1) and (1×2) surfaces.[144]

3.3.2 Carbon monoxide adsorption on Pt(110)

While the CO adsorption on reactive surfaces such as alkali and rare earth metals is normally dissociative [129], on d-metal surfaces (e.g. Cu, Ag) it is predominantly molecular, and the strength of the CO–metal bond is relatively weak. In fact, by increasing the temperature of the substrate CO desorbs molecularly before dissociatiating. For the majority of the transition metals, however, the nature of the adsorption is very sensitive to the temperature and the structure of the surface.

On the Pt(110) surface CO adsorbs in a molecular form. The CO bonding on Pt as well as on other transition metal surfaces is explained by the Blyholder model [145], originally developed for metal carbonyl systems [146]. The 5σ and the 2π frontier molecular orbitals (MO) of the CO molecule are substantially modified by the presence of the metal surface (Figure 3.9 [147]). A filled 5σ "lone pair" orbital interacts with the empty ds metal orbitals, leading to a partial transfer of electron density to the metal. At the same time the filled metal dp orbitals overlap with the 2π* antibonding molecular orbital of the CO (Figure 3.10).

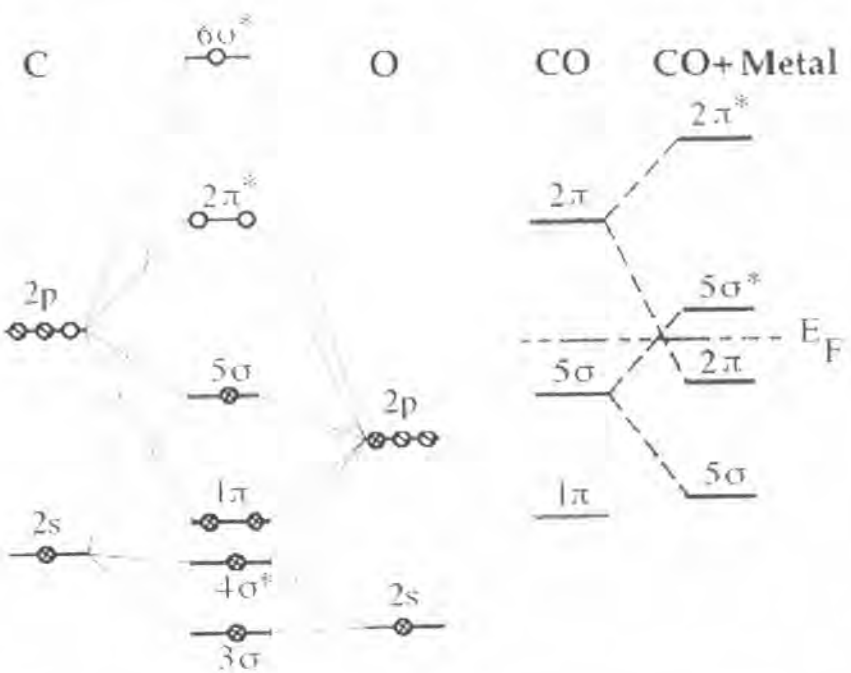

Figure 3.9 MO diagram for a CO–metal system [147].

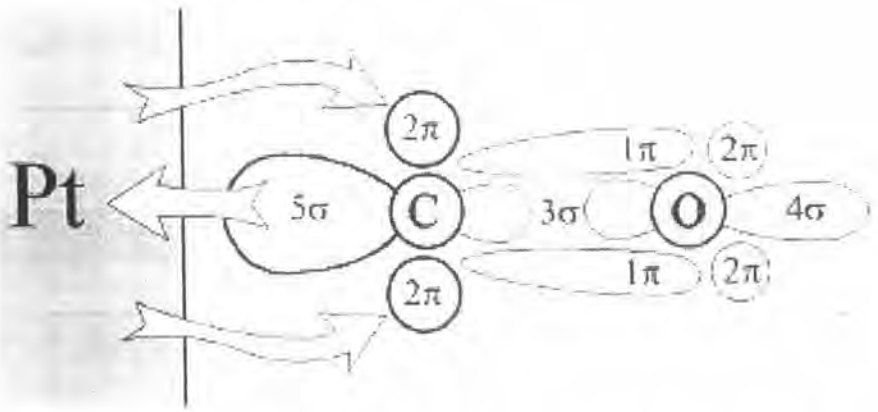

Figure 3.10 The donation-backdonation mechanism [148].

Since in the course of this electron donation-backdonation process antibonding orbitals are populated, the strength of the carbon–oxygen bond [148] and, as a consequence, the stretching frequency [149] are lowered, compared to the isolated molecule in the gas phase. Moreover, since the 5σ and 2π MO of CO are localized mainly at the C atom, the bonding occurs with the carbon atom facing the surface.

3.3.3 Oxygen on Pt(110)

On a Pt(110) surface oxygen adsorbs molecularly at T < -153 °C and issociatively at higher temperature [150]. At 27 °C oxygen adsorbs initially on the 4-fold coordinated sites located at the bottom of the (110) valleys [151]. At higher exposures even the 3-fold (111) nanofacets, in Figure 3.11 [152], start to be populated. Other authors instead favor, the occupation of the site at the walls of the troughs [153]. The saturation coverage at 27 °C is estimated to be 0.35 ml [154], in agreement with the recent results of Walker et al. [153]. In the latter article the authors also report a value of 0.4 for the initial sticking coefficient at 27 °C.

At about 527 °C recombinative molecular desorption takes place (Figure 3.12 [155]). The dissociation of oxygen on metal surfaces has been modeled by abinitio fully quantum-dynamical simulations [151, 156]. The role of the electronic energy states in the dissociative adsorption of O_2 has been studied by Heiz and coworkers [157] by varying the size of Pt clusters, and, in turn, the position of the d-band. They found that oxygen dissociation occurs preferentially on those clusters whose states induce enough

backdonation into the antibonding $2\pi_g^*$ state or a sufficient donation from the $1\pi_u$ or $5\sigma_g$ oxygen molecular orbitals into the cluster. Both processes, in fact, reduce the bond order of the oxygen molecule. On the Pt(110) surface oxygen atoms diffuse preferentially along the (110) direction [158]. The macroscopic diffusion coefficient, strongly dependent on the oxygen coverage, is on the order of 10^{-8} $cm^2 \cdot s^{-1}$ at 327 °C.

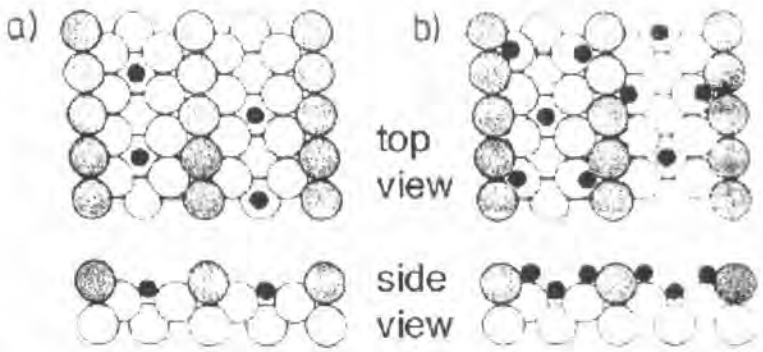

Figure 3.11 O/ Pt(110): a) low and b) high coverage [152].

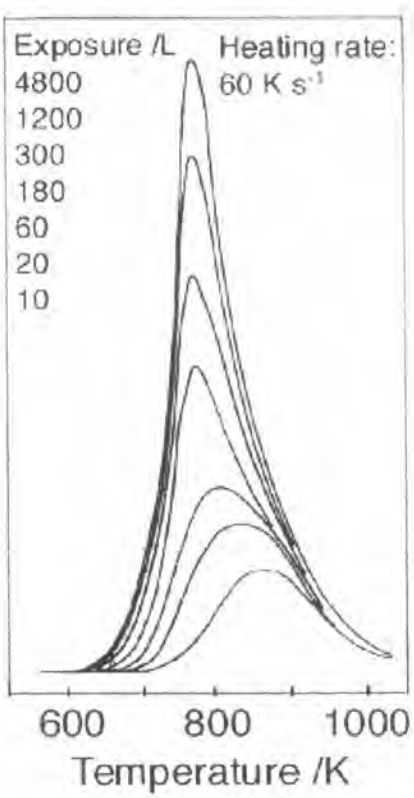

Figure 3.12 TD data of O_2/Pt(110) [155]

3.3.4 Surface reconstruction mechanism

Two different phases of the Pt(110) surface can be observed, depending on the preparation procedure. Right after Ar ions sputtering a metastable (1×1), disordered structure can be observed, which converts within a short time into the (1×2) structure. An adsorbate-induced lifting of the (1×2) surface reconstruction occurs upon CO adsorption, starting at a CO coverage of 0.2 ml. Moreover, under appropriate reaction conditions, a faceting of the Pt(110) surface is reported at temperature below 227 °C [159]. These facets consist of steps and terraces in the (001) direction with a spatial periodicity on the order of 100 Å. The (1×2) is destabilized above 627 °C, as displayed by a blurry (1×1) LEED pattern [160].

It is notable that in order to transform the ordered missing row into an ideal bulkterminated structure (Figure 3.8), an extensive mass transport, involving a substantial rearrangement of a large part of the surface Pt atoms, is needed. The key point for the interpretation is that the diffraction pattern [161] of the deconstructed [162] CO/Pt(110) (1×1) surface does not correspond to an ordered structure but rather to a strongly disordered system. A similar behavior was found for NO/Pt(110) [163].

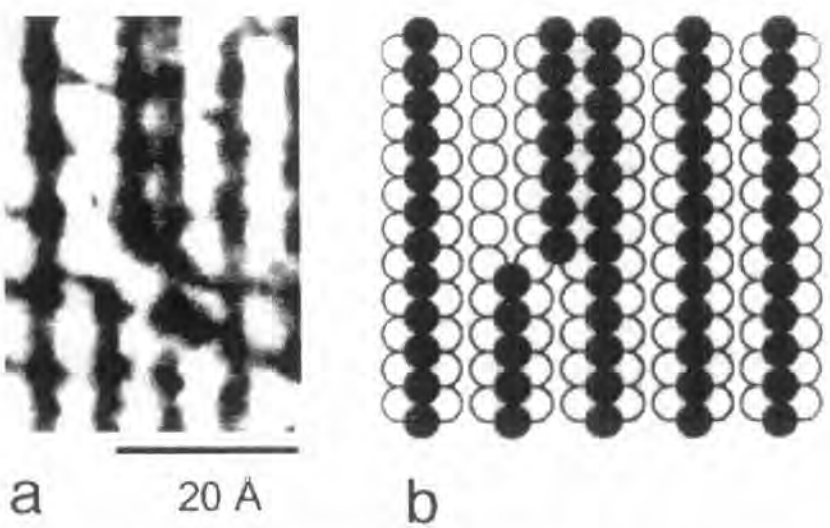

Figure 3.13 The row pairing mechanism; a) an STM image;
b) a schematic model [164].

It was observed (Figure 3.13a [164]) that the transition occurs locally by displacing single Pt atoms from (1×2) sites. Therefore, in what appears as an order-disorder transition, Pt atoms of the first layer begin to diffuse out of the $(1\bar{1}0)$ rows and occupy lattice sites without (1×2) periodicity. At high CO coverages the atoms are randomly distributed on all possible lattice sites determined by the bulk. At this point the diffraction pattern is indistinguishable from the one of a perfectly ordered (1×1) surface. As a result, additional sites in the second platinum atomic layer start to be accessible for the adsorption, which accounts for the increased oxygen sticking probability on the (1×1) surface.

3.3.5 O_2 and CO on Pt(110): the reaction

It is now widely accepted that the reaction proceeds via the Langmuir-Hinshelwood mechanism [165]. Both reactants adsorb on the catalyst surface in order to yield the product. The reaction centers of the metal are the coordination-unsaturated surface atoms with underpopulated d orbitals. The reaction steps are:

$$CO(g) + \otimes \leftrightarrow CO_{AD} \tag{3.6}$$

$$O_2(g) + \otimes\text{-}\otimes \rightarrow 2O_{AD} \tag{3.7}$$

$$CO_{AD} + O_{AD} \rightarrow CO_2(g) + \otimes\text{-}\otimes \tag{3.8}$$

They correspond to the molecular and dissociative adsorption of CO and O_2, respectively, and the subsequent diffusion of a CO towards an oxygen atom, followed by the production of CO_2, which immediately leaves the surface. Since oxygen needs two adjacent free sites (indicated with ⊗-⊗) for the chemisorption, the coadsorption characteristics of the two species are quite different, depending on the sequence of the adsorption: a phenomenon named asymmetric inhibition (Figure 3.14). While at all oxygen coverages there is still enough place to accommodate CO molecules, oxygen adsorption is completely blocked by carbon monoxide already at a coverage of 0.3 ml due to the lack of available pairs of neighbor sites. The observed [150] increase of the oxygen sticking probability on the (1×1) surface looks puzzling, since the CO at the concentration required to lift the reconstruction is expected to inhibit any oxygen adsorption.

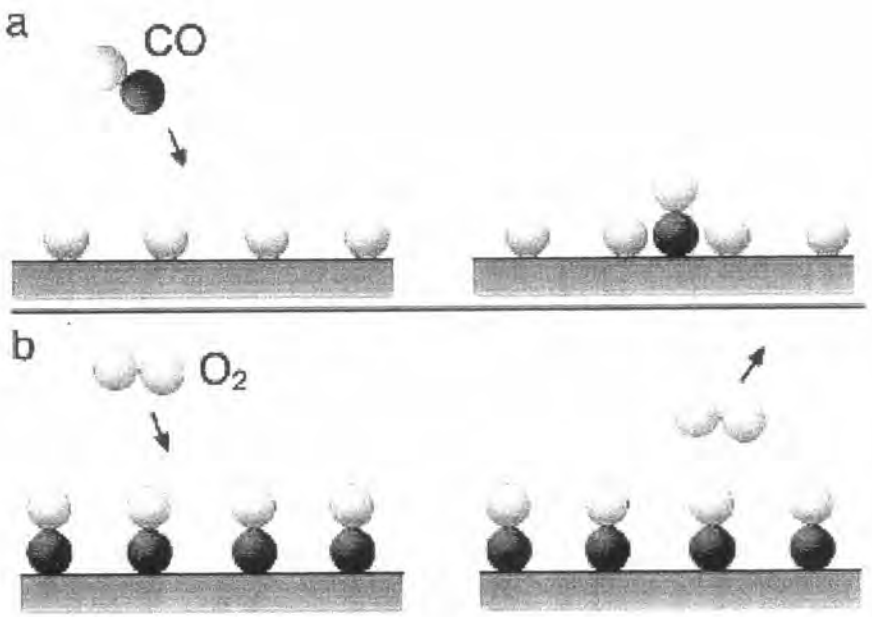

Figure 3.14 The asymmetric inhibition. a) CO adsorption on a oxygen precovered surface; b) O_2 adsorption on a CO predosed surface [165].

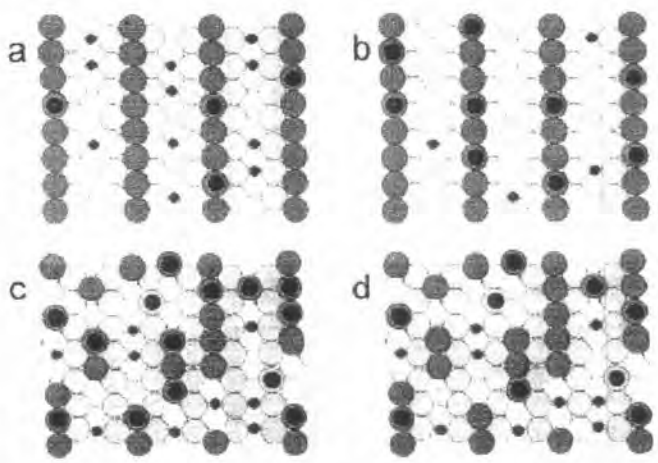

Figure 3.15 Schematic of the reaction cycle [165].

Figure 3.15 (a) shows how on a prevalently O covered surface the CO adsorbs and reacts easily forming CO_2, consuming the oxygen (b), until the critical coverage necessary to lift the reconstruction is reached (c). New highly coordinated empty sites, created in the course of the process, favor oxygen adsorption and reaction, consuming CO. The CO concentration falls (d), restarting the cycle.

An increase of the catalytic activity, interpreted as an increased oxygen sticking probability, was observed in correlation with the process of faceting of the surface during the reaction at temperature between 127 and 227 °C [159]. In such cases, instead of oscillations, a continuous rise of the CO_2 production rate has been observed.